Nanoscale Research Letters
a SpringerOpen Journal

NANO EXPRESS Open Access

Grain size-dependent magnetic and electric properties in nanosized $YMnO_3$ multiferroic ceramics

Tai-Chun Han*, Wei-Lun Hsu, Wei-Da Lee

Abstract

Magnetic and electric properties are investigated for the nanosized $YMnO_3$ samples with different grain sizes (25 nm to 200 nm) synthesized by a modified Pechini method. It shows that magnetic and electric properties are strongly dependent on the grain size. The magnetic characterization indicates that with increasing grain size, the antiferromagnetic (AFM) transition temperature increases from 52 to 74 K. A corresponding shift of the dielectric anomaly is observed, indicating a strong correlation between the electric polarization and the magnetic ordering. Further analysis suggests that the rising of AFM transition temperature with increasing grain size should be from the structural origin, in which the strength of AFM interaction as well as the electrical polarization is dependent on the in-plane lattice parameters. Furthermore, among all samples, the sample with grain size of 95 nm is found to have the smallest leakage current density (< 1 μA/cm^2).

PACS: 75.50.Tt, 75.50.Ee, 75.85.+t, 77.84.-s

Introduction

The hexagonal $RMnO_3$ (R = rare earth element or Y) compounds present opportunities for the industrial applications due to their unique nature of multiferroism [1]. Namely, the ferromagnetism, ferroelectricity and ferroelasticity occur simultaneously in the same material. The characteristics of multiferroism include a spontaneous magnetization which can be switched by an applied electric field, a spontaneous electrical polarization which can be reoriented by an applied magnetic field, and a strong coupling between these two properties [2]. Owing to the coupling between ferroelectric and magnetic domains, multiferroism is likely to offer a whole range of new applications and phenomena. Specific device applications that have been proposed for these multiferroic materials include the multiple-state memory elements, the transducer with magnetically modulated piezoelectricity, and the electric-field-controlled ferromagnetic resonance devices [2].

Most of hexagonal $RMnO_3$ exhibit ferroelectric (FE) transitions at high temperatures ($T_C \approx 600$ to 1,000 K) and antiferromagnetic (AFM) transitions at low temperatures ($T_N \approx 70$ to 130 K) with a frustrated triangular arrangement of Mn spins in the hexagonal c-plane [1-4]. Additional phase transitions at the temperature below 10 K were observed in the hexagonal $RMnO_3$ with the R^{3+} ion of high magnetic moment, which is related to the R-R exchange correlations [5]. Several attempts have been directed towards the syntheses of new $RMnO_3$ compounds and the studies of their related properties [6,7]. In particular, the recent work on the hexagonal $RMnO_3$ compounds was focused on the following subjects: (1) the magnetic phases and the magnetic symmetry at low temperatures [8,9], (2) the coupling between the magnetic and FE orderings [10,11], and (3) the strong spin-lattice interaction of the geometrically frustrated Mn-spin system [12]. The studies on $YMnO_3$, $HoMnO_3$ and $LuMnO_3$ indicated that the values of ordering temperatures are associated with the size of R^{3+} ion. In addition, the size effects in yttrium-based manganites were also reported [13,14]. However, the size effects on the multiferroism remain unclear, and its understanding requires more experimental evidences. In this paper, we prepare a series of $YMnO_3$ samples with different grain sizes by a modified Pechini method to study systematically the effect of grain size on their magnetic and electric properties.

Experimental procedure

The nanosized samples of $YMnO_3$ were synthesized by a modified Pechini method using nitrates as metal precursors. First, yttrium nitrate [$Y(NO_3)_3{\cdot}6H_2O$] and manganese nitrate [$Mn(NO_3)_2{\cdot}4H_2O$] in stoichiometric proportions

* Correspondence: tchan@nuk.edu.tw
Department of Applied Physics, National University of Kaohsiung, Kaohsiung 811, Taiwan

(1:1 molar ratio) were dissolved in distilled water. Citric acid ($C_6H_8O_7$) in 1:1 molar ratio with respect to the metal nitrates was added to the solution as a complexant, and the solution was adjusted to a PH value of 6.5 to 7 by adding ammonia. The mixture was dried at 120°C to form a gel, and then the obtained gel was burned until the combustion process was completed. After that, the precursory powders were reground and pressed into the pellets. Finally, the pellets were sintered at different temperatures ranging from 800°C to 1,050°C for 2 h, respectively. Electrodes were applied to both surfaces to measure electrical properties with silver paste.

The crystalline structure and the phase purity of the samples were examined with a typical X-ray diffraction (XRD), acquired by a Bruker D8 Advance X-ray diffractometer (Bruker UK Ltd., Coventry, Warwickshire, UK) equipped with a monochromatized Cu $K_{\alpha 1}$ radiation and field emission scanning electron microscopy. The magnetization was measured with a Quantum Design superconducting quantum interference device (Quantum Design, Inc., San Diego, CA, USA) with an applied magnetic field of 500 Oe. For the dielectric measurements, a capacitance bridge (Agilent 4284A; Agilent Technologies, Inc., Palo Alto, CA, USA) hooked to a probe station with a closed-cycle low temperature system was used. The leakage currents of the samples were measured using a commercial FE test system (TF Analyzer, aixACCT Systems GmbH, Aachen, Germany).

Results and discussion

Figure 1 shows the XRD patterns of the $YMnO_3$ samples sintered at different temperatures from 800°C to 1,050°C. Based on the standard reference, all the observed peaks can be indexed on the basis of a hexagonal unit cell of space group $P6_3cm$ (JCPDS:25-1079), suggesting that all samples are pure phases without any impurity. In addition, with the increase in sintering temperature, there is a gradual intensity increasing and narrowing of the diffraction peaks, indicative of better crystallization and the grain growth. The lattice parameters were determined by Rietveld refinement method and shown in Figure 2. With increasing of sintering temperature, the value of c lattice parameter is slightly expanded, while the value of a lattice parameter decreased. The typical scanning electron microscopy (SEM) images of the $YMnO_3$ samples sintered at different temperatures are shown in Figure 3. From the images, it can be found that the grain size becomes larger as the sintering temperature increases. The estimated average grain size is about 25, 45, 95, and 200 nm for the samples sintered at 800°C, 850°C, 900°C, and 1,050°C, respectively.

The temperature-dependent magnetization curves M (T) were measured in a magnetic field of 500 Oe under the conditions of zero-field-cooled (ZFC) and field-cooled (FC). Figure 4 displays the temperature dependence of magnetization for the powders with different grain sizes. Open symbols are the data with the ZFC mode, while the solid ones with FC mode. As can be seen, typical AFM to paramagnetic (PM) phase transition is observed for the sample with grain size of 200 nm, and the Néel temperature (T_N) is about 74 K. As the grain size decreases, the value of T_N shifts to the lower temperatures and is equal to 52 K for the sample with grain size of 25 nm. This size-dependent T_N is similar to the observation in the $BiFeO_3$ nanoparticles [15], where the increase in T_N with increasing size has been discussed both in terms of phenomenological scaling relations and possible correlations with the decreasing electrical polarization. To further explore the magnetic properties of the samples, magnetic hysteresis loops for the $YMnO_3$ samples with different grain sizes have been measured at 5 K, as presented in Figure 5. For the samples with grain size of 25 and 45 nm, weak ferromagnetic (FM) behavior is observed with corresponding coercivity (Hc) about 395 and 260 Oe, respectively. The inset in Figure 5 shows the magnetic hysteresis curve for the sample with grain size of 25 nm has been measure at 55 K. It indicates the PM behavior which confirms that the FM component disappears above T_N. Therefore, the weak FM component does not come from FM impurity phase. As the grain size increases, the weak FM behavior transforms into paramagnetism. Similar effect of grain size on magnetism was also reported in nanosized YMn_2O_5 [16] and $BiFeO_3$ particles [17]. In fact, weak surface FM component is a universal feature for nanosized AFM systems, which is attributed to the deviation of the AFM arrangement to the disordered surface spin due to the lattice strain [17,18]. Based on the above consideration, the magnetic structure of the nanosized $YMnO_3$ can be considered as a core/shell system, where the inner part of the particle is AFM phase and the surface is FM component.

Figure 6 shows the temperature-dependent dielectric permittivity $\varepsilon(T)$ and loss tangent ($\tan\delta$) at 100 kHz for all measured $YMnO_3$ samples. In Figure 6a, the dielectric anomalies are observed at T^* which is defined as the crossing point of two slopes as indicated by arrows. It shows that the T^* shifts from 55 to 74 K with increasing grain sizes from 25 to 200 nm. As clearly apparent in Figure 6b, the positions of the broad peaks for the $YMnO_3$ samples with different grains sizes are near their T^*. Moreover, the enhanced dielectric response observed for $YMnO_3$ with larger grains is similar to previously reported results for $BaTiO_3$ dielectrics [19]. The observed systematic shift in the temperatures of magnetic transition and dielectric anomaly demonstrates a strong correlation between magnetic ordering and electric polarization in nanosized

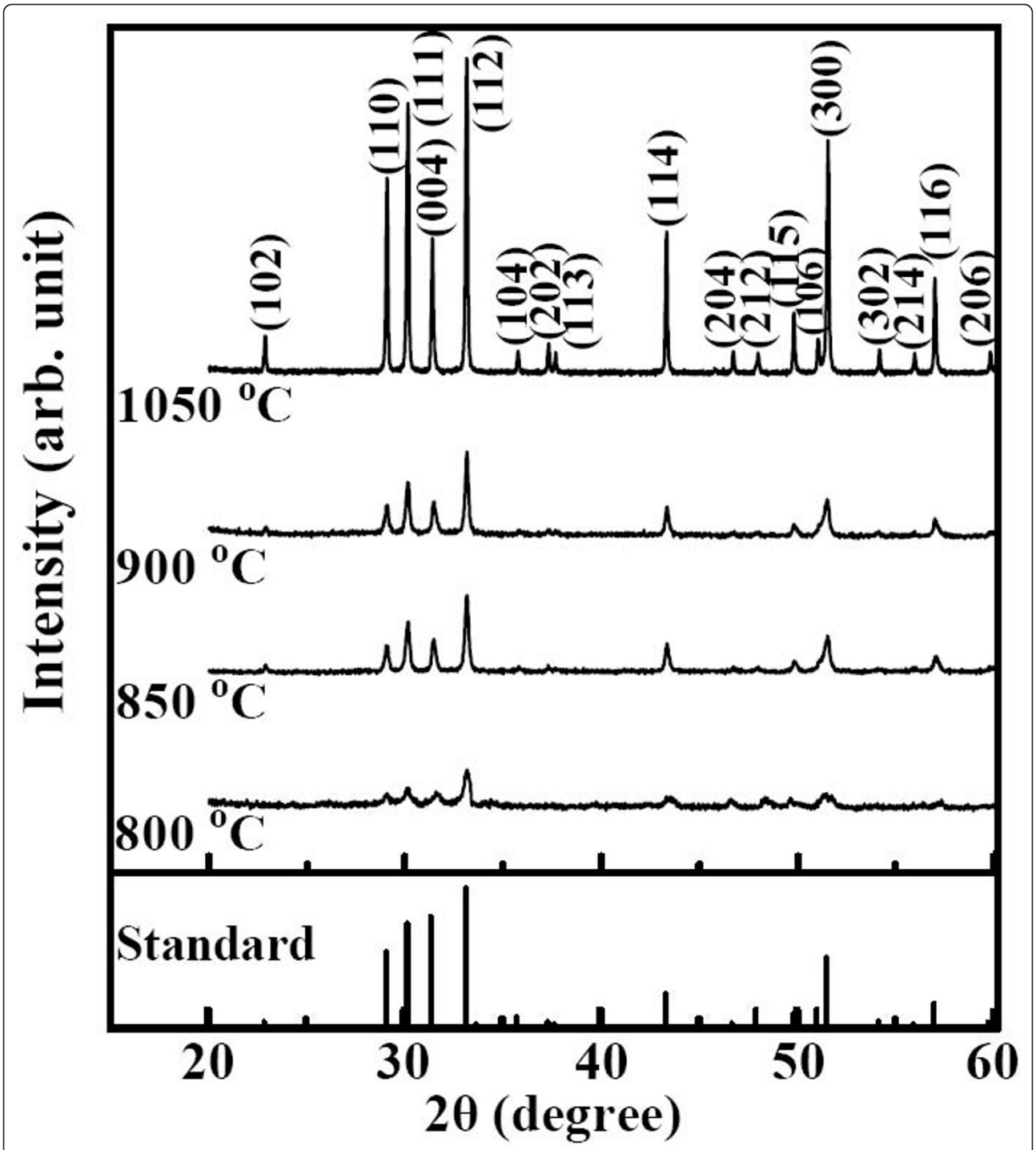

Figure 1 The standard reference and the XRD patterns of $YMnO_3$ samples sintered at different temperatures. Samples were sintered at temperatures ranging from 800°C to 1,050°C for 2 h, respectively.

hexagonal $YMnO_3$ ceramics. As to the coupling between antiferromagnetism and dielectric property, Katsufuji et al. [20] suggested that the dielectric anomaly was caused by the magnetic-ordering-dependent electronic excitation gap E_g in *ab*-plane. According to this model, the change of AFM ordering pattern can induce dielectric anomaly via the change of E_g, in a formula of $\varepsilon = 1/E_g^2$. Therefore, one can understand that the shift in the temperature of dielectric anomalies is related to the AFM interaction through the variation of Mn-O bond length with change the lattice

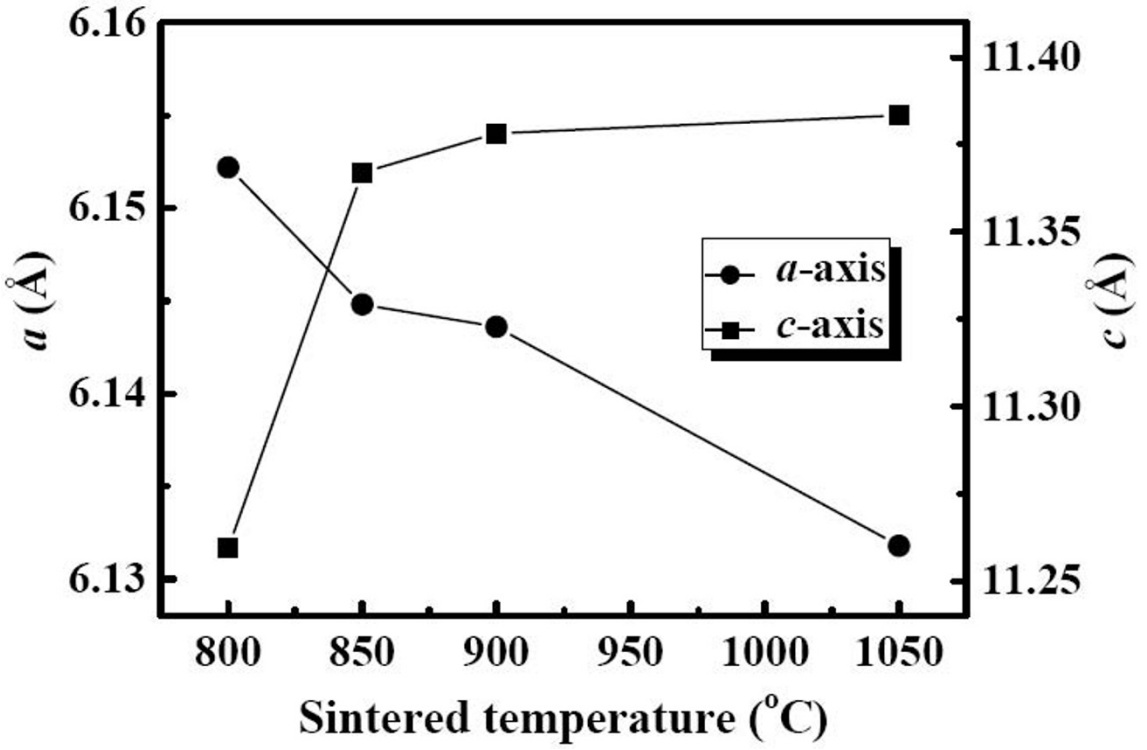

Figure 2 The evolution of lattice parameters for $YMnO_3$ samples sintered at different temperatures. The uncertainty is contained within the area of the suitable mark.

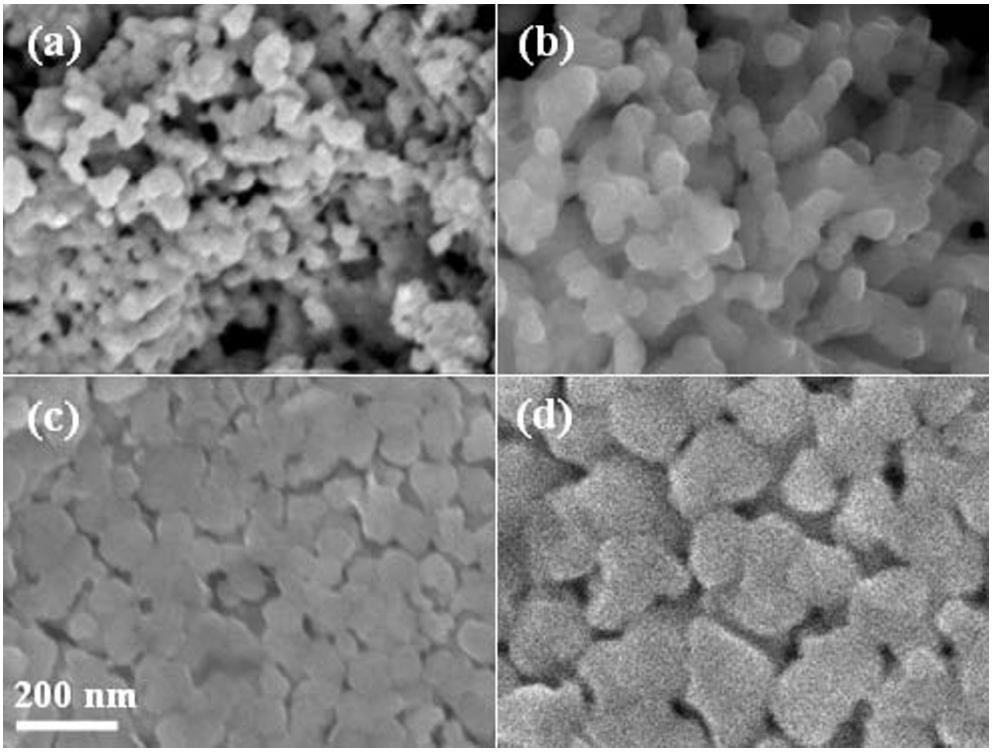

Figure 3 The SEM micrographs for $YMnO_3$ samples. Samples sintered at **(a)** 800°C, **(b)** 850°C, **(c)** 900°C, and **(d)** 1,050°C, respectively.

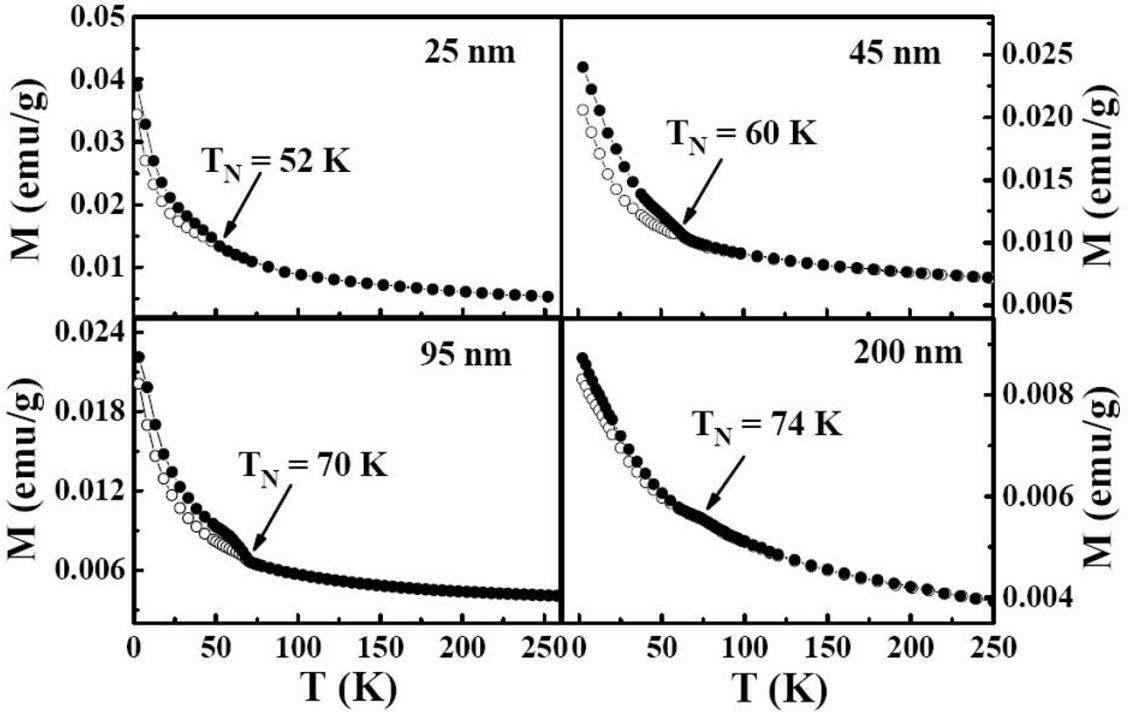

Figure 4 Temperature dependence of magnetization for the $YMnO_3$ samples with different grain sizes. Open symbols are the data with the ZFC while the solid ones with FC mode.

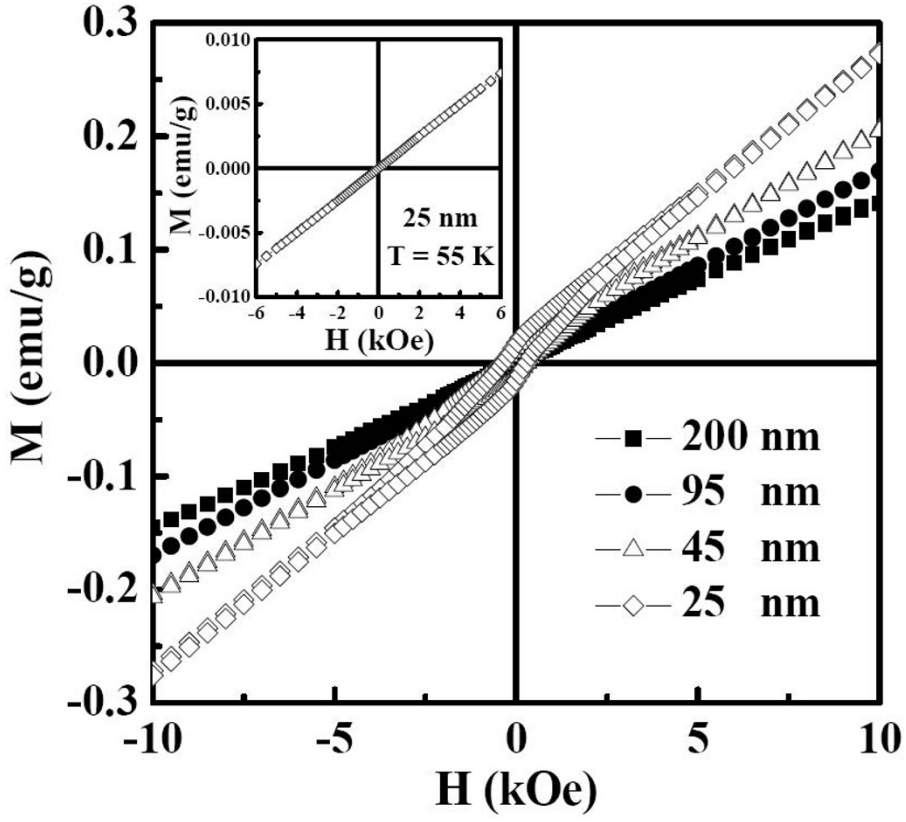

Figure 5 Magnetic hysteresis loops at 5 K for the $YMnO_3$ samples with different grain sizes. Inset: magnetic hysteresis curve at 55 K for the sample with grain size of 25 nm.

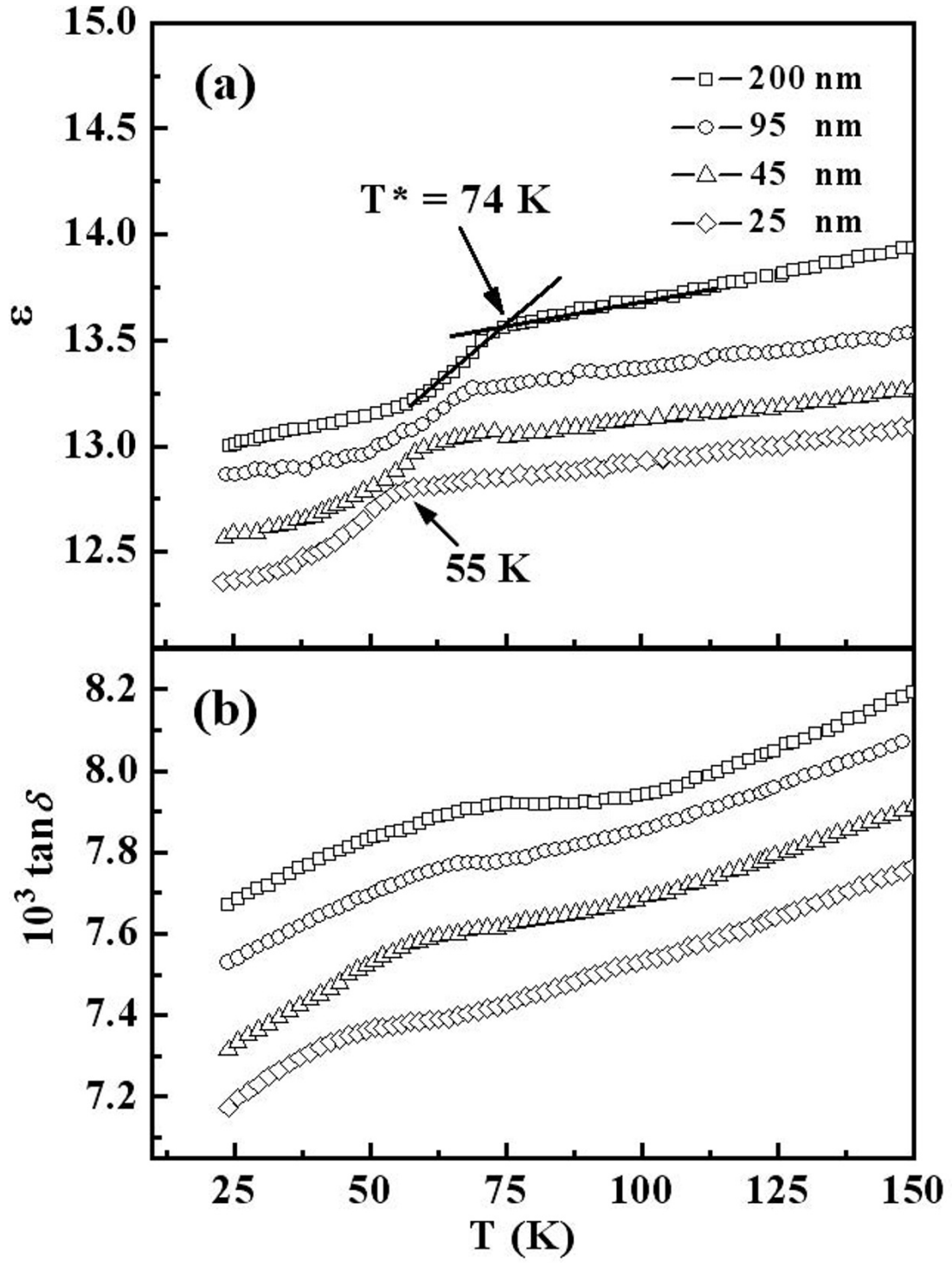

Figure 6 Temperature-dependent (a) dielectric constant (ε), and (b) loss tangent for the $YMnO_3$ samples. Samples have different grain sizes (25 nm to 200 nm).

parameters. In addition, the systematical change in the lattice constant *a* plays an important role since the strength of AFM interactions strongly depends on the bond length of Mn-O. In general, the strength of AFM interaction can be written as [21]:

$$I = \frac{1}{2}J\sum \hat{S}_i \cdot \hat{S}_j \quad (1)$$

where the sum is over the nearest neighbors and $\hat{S}_i$ is a spin operator. The parameter *J* is proportional to the inverse of the distance between two nearest spins. Therefore, the reduction in *a*-parameter leads to the enhancement of *J* and hence to the rising of AFM transition temperature.

To further probe the electrical leakage effect, the leakage current were measured for all the samples at room temperature as shown in Figure 7. The leakage current density is large (> 100 μA/cm^2) for the sample with grain size of 25 nm. On the other hand, the leakage currents are much decreased by about four orders of magnitude for the samples with grain size larger than 45 nm. In addition, it is not expected that the sample with larger grain size of 200 nm is not the less leaky sample. As for the improvement of the leakage properties, it should be associated with the high denseness of the ceramics [22].

Conclusions

In summary, a series of hexagonal $YMnO_3$ samples with different grain sizes are synthesized by a modified Pechini method. The magnetic susceptibility indicates that with increasing grain size from 25 to 200 nm, the AFM transition temperature increases from 52 to 74 K. At the same time, a corresponding shift of the dielectric anomalies is observed, which suggests a strong

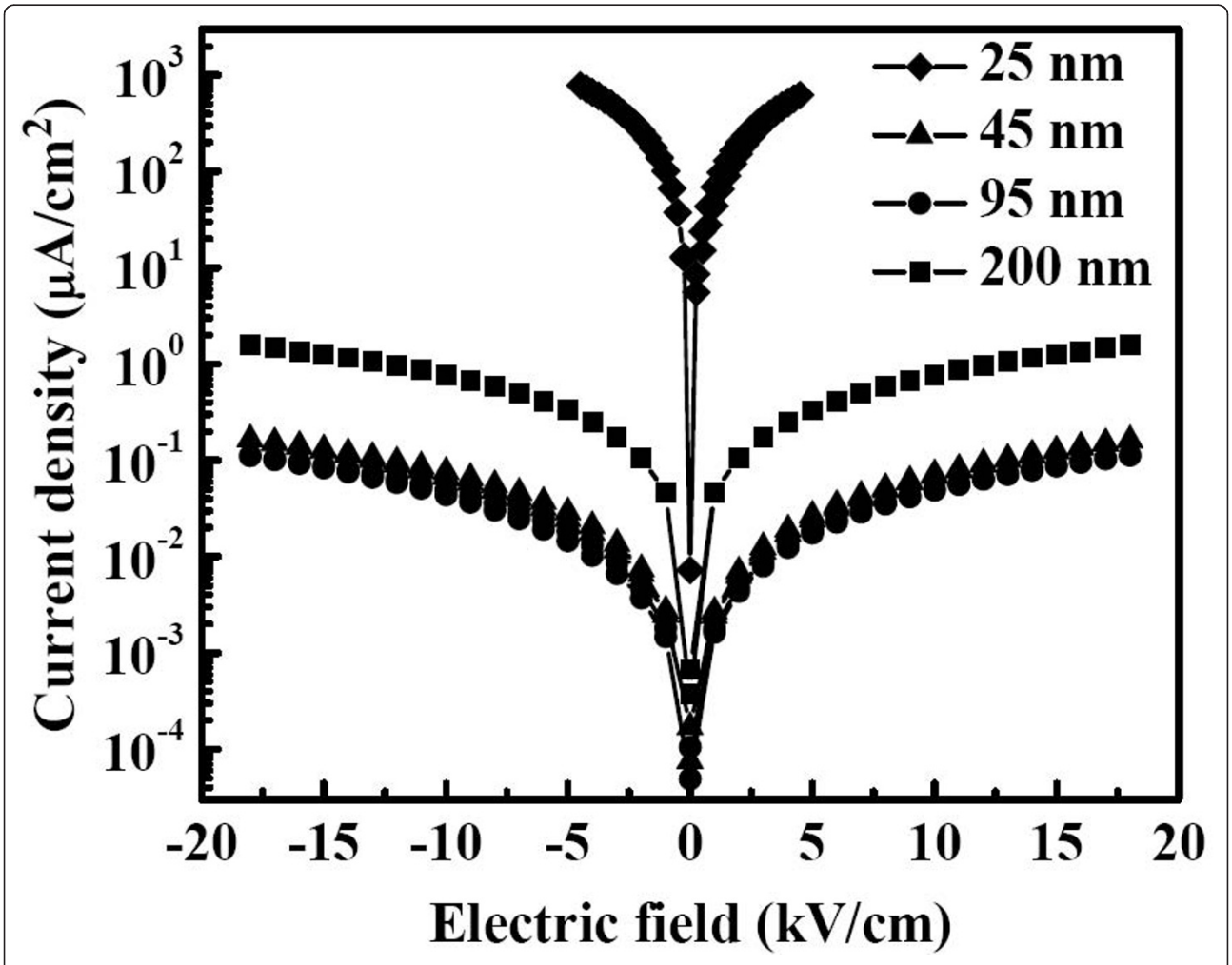

Figure 7 Leakage current as function of applied electric field for the $YMnO_3$ samples. Samples have different grain sizes (25 nm to 200 nm).

correlation between the magnetic ordering and the electric polarization. Since the electronic excitation gap is inversely proportional to the dielectric permittivity and the spin structure influences the electronic excitation gap, we propose that the coherent shift in the magnetic ordering and the dielectric anomalies to high temperature with increasing grain size is related to the suppression of the in-plane lattice parameter.

Acknowledgements
The financial support of this work is from the National Science Council of Taiwan under the grant nos. NSC96-2112-M-390-003-MY3, 99-2112-M-390-005-MY3 and 98-2815-C-390-015-M.

Authors' contributions
The work presented here was carried out in collaboration between all authors. TH defined the research theme and designed methods and experiments, carried out the laboratory experiments, analyzed the data, interpreted the results and wrote the paper. WH and WL prepared the samples, helped to carry out the laboratory experiments and discussed analyses. All authors read and approved the final manuscript.

Competing interests
The authors declare that they have no competing interests.

Received: 26 July 2010 Accepted: 8 March 2011
Published: 8 March 2011

References

1. Van Aken BB, Palstra TTM, Filippetti A, Spaldin NA: **The origin of ferroelectricity in magnetoelectric $YMnO_3$.** *Nat Mater* 2004, **3**:164.
2. Fiebig M: **Revival of the magnetoelectric effect.** *J Appl D: Appl Phys* 2005, **38**:R123.
3. Bertaut EF, Forrat EF, Fang P: **A new class of ferroelectric: rare earth and yttrium manganites.** *Acad Sci* 1963, **256**:1958.
4. Choi T, Horibe Y, Yi HT, Choi YJ, Wu W, Cheong SW: **Insulating interlocked ferroelectric and structural antiphase domain walls in multiferroic $YMnO_3$.** *Nat Mater* 2010, **9**:253.
5. Fiebig M, Lottermoser Th, Pisarev RV: **Spin-rotation phenomena and magnetic phase diagrams of hexagonal $RMnO_3$.** *J Appl Phys* 2003, **93**:8194.
6. Floros N, Rijssenbeek JT, Martinson AB, Poeppelmeier KR: **Structural study of A_2CuTiO_6 (A = Y, Tb-Lu) compounds.** *Solid State Sci* 2002, **4**:1495.
7. Malo S, Maignan A, Marinel S, Hervieu M, Poeppelmeier KR, Raveau B: **Structural and magnetic properties of the solid solution ($0 \le \times \le 1$) $YMn_{1-x}(Cu_{3/4}Mo_{1/4})_xO_3$.** *Solid State Sci* 2005, **7**:1492.
8. Fiebig M, Fröhlich D, Kohn K, Leute St, Lottermoser Th, Pavlov VV, Pisarev RV: **Determination of the magnetic symmetry of hexagonal manganites by second harmonic generation.** *Phys Rev Lett* 2000, **84**:5620.
9. Muñoz A, Alonso JA, Martínez-Lope MJ, Casáis MT, Martínez JL, Fernández-Díaz MT: **Evolution of the magnetic structure of hexagonal $HoMnO_3$ from neutron powder diffraction data.** *Chem Mater* 2001, **13**:1497.
10. Huang ZJ, Cao Y, Sun YY, Xue YY, Chu CW: **Coupling between the ferroelectric and antiferromagnetic orders in $YMnO_3$.** *Phys Rev B* 1997, **56**:2623.
11. Sugie H, Iwata N, Kohn K: **Magnetic ordering of rare earth ions and magnetic-electric interaction of hexagonal $RMnO_3$ (R = Ho, Er, Yb or Lu).** *J Phys Soc Jpn* 2002, **71**:1558.
12. Zhou HD, Lu J, Vasic R, Vogt BW, Janik JA, Brooks JS, Wiebe CR: **Relief of frustration through spin disorder in multiferroic $Ho_{1-x}Y_xMnO_3$.** *Phys Rev B* 2007, **75**:132406.
13. Zhang MF, Liu JM, Liu ZG: **Microstructural characterization of nanosized $YMnO_3$ powders: the size effect.** *Appl Phys A* 2004, **79**:1753.
14. Zheng HW, Liu YF, Zhang WY, Liu SJ, Zhang HR, Wang KF: **Spin-glassy behavior and exchange bias effect of hexagonal $YMnO_3$ nanoparticles fabricated by hydrothermal process.** *J Appl Phys* 2010, **107**:053901.
15. Selbach SM, Tybell T, Einarsrud MA, Grande T: **Size-dependent properties of multiferroic $BiFeO_3$ nanoparticles.** *Chem Mater* 2007, **19**:6478.
16. Ma C, Yan JQ, Dennis KW, McCallum RW, Tan X: **Size-dependent magnetic properties of high oxygen content $YMn_2O_{5\pm\delta}$ multiferroic nanoparticles.** *J Appl Phys* 2009, **105**:033908.
17. Bi H, Li SD, Zhang YC, Du YW: **Ferromagnetic-like behavior induced by lattice distortion of ultrafine NiO nanocrystallites.** *J Magn Magn Mater* 2004, **277**:363.
18. Bañdobre-Lopez M, Vázquez-Vázquez C, Rivas J, López-Quintela MA: **Magnetic properties of chromium (III) oxide nanoparticles.** *Nanotechnology* 2003, **14**:318.
19. Ihlefeld JF, Vodnick AM, Baker SP, Borland WJ, Maria JP: **Extrinsic scaling effects on the dielectric response of ferroelectric thin films.** *J Appl Phys* 2008, **103**:074112.
20. Katsufuji T, Mori S, Masaki M, Moritomo Y, Yamamoto N, Takagi H: **Dielectric and magnetic anomalies and spin frustration in hexagonal $RmnO_3$ (R = Y, Yb, and Lu).** *Phys Rev B* 2001, **64**:104419.
21. Munawar I, Curnoe SH: **Theory of magnetic phases of hexagonal rare earth manganites.** *J Phys: Condens Matter* 2006, **18**:9575.
22. Chen F, Zhang QF, Li JH, Qi YJ, Lu CJ, Chen XB, Ren XM, Zhao Y: **Sol-gel derived multiferroic $BiFeO_3$ ceramics with large polarization and weak ferromagnetism.** *Appl Phys Lett* 2006, **89**:092910.

doi:10.1186/1556-276X-6-201
Cite this article as: Han *et al.*: Grain size-dependent magnetic and electric properties in nanosized $YMnO_3$ multiferroic ceramics. *Nanoscale Research Letters* 2011 **6**:201.